Letter

Equilibrium Potential of Free Charge Carriers in a Bent Piezoelectric Semiconductive Nanowire

Yifan Gao, and Zhong Lin Wang

Nano Lett., **2009**, 9 (3), 1103-1110• DOI: 10.1021/nl803547f • Publication Date (Web): 03 February 2009

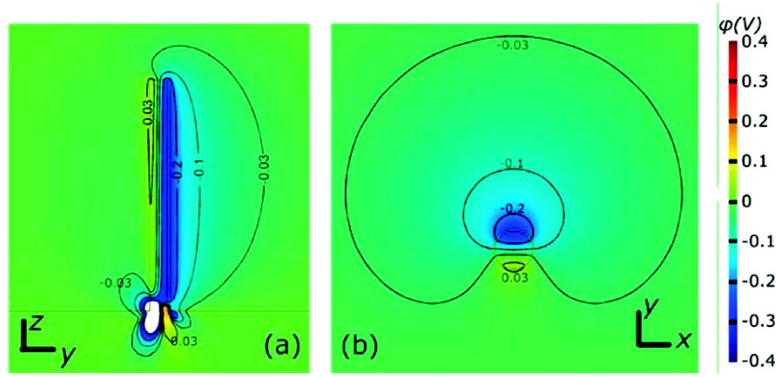

More About This Article

Additional resources and features associated with this article are available within the HTML version:

- Supporting Information
- Access to high resolution figures
- Links to articles and content related to this article
- Copyright permission to reproduce figures and/or text from this article

View the Full Text HTML

NANO LETTERS

2009
Vol. 9, No. 3
1103-1110

Equilibrium Potential of Free Charge Carriers in a Bent Piezoelectric Semiconductive Nanowire

Yifan Gao and Zhong Lin Wang*

School of Materials Science and Engineering, Georgia Institute of Technology, Atlanta Georgia 30332-0245

Received November 23, 2008; Revised Manuscript Received December 31, 2008

ABSTRACT

We have investigated the behavior of free charge carriers in a bent piezoelectric semiconductive nanowire under thermodynamic equilibrium conditions. For a laterally bent n-type ZnO nanowire, with the stretched side exhibiting positive piezoelectric potential and the compressed side negative piezoelectric potential, the conduction band electrons tend to accumulate at the positive side. The positive side is thus partially screened by free charge carriers while the negative side of the piezoelectric potential preserves as long as the donor concentration is not too high. For a typical ZnO nanowire with diameter 50 nm, length 600 nm, donor concentration $N_D = 1 \times 10^{17}$ cm^{-3} under a bending force of 80 nN, the potential in the positive side is <0.05 V and is approximately −0.3 V at the negative side. The theoretical results support the mechanism proposed for a piezoelectric nanogenerator. Degeneracy in the positive side of the nanowire is significant, but the temperature dependence of the potential profile is weak for the temperature range of 100−400 K.

Introduction. Nanowires (NWs) and nanobelts made of wurtzite-structured compound semiconductors, such as ZnO and GaN,[1,2] are piezoelectric. By use of the piezoelectricity of semiconductive ZnO NWs, nanoscale mechanical−electrical energy conversion devices known as the nanogenerators have been demonstrated,[3−7] in which the electric current in an external circuit is driven by the piezoelectric potential created by the bent ZnO NW.[7] On the basis of the coupled behavior between piezoelectric and semiconducting properties, piezotronic effect[8] has been revealed, which utilizes the piezoelectric potential to modulate the carrier transport process in the NW. Examples of nanopiezotronics include but are not limited to the piezoelectric field effect transistors,[8] piezoelectric diodes,[9] and piezotronic strain sensors.[10] Although most of the nanogenerators and nanopiezotronics devices are based on ZnO NWs and nanobelts, the demonstrated principle applies to a broad range of materials, such as GaN, CdS, and possibly ZnS.

Nanowires and nanobelts are natural cantilevers that can be easily bent to create a large deformation. Although the application of piezoelectricity in semiconductor devices has a long history in the GaN/AlGaN high electron mobility transistors (HEMTs),[11,12] the piezoelectric fields in traditional HEMTs are fixed as introduced by interface strain and remain "as is" once the heterojunctions are fabricated. In contrast, the mechanical flexibility of piezoelectric compound nanowires provides a more versatile platform to utilize the physics of piezoelectricity in semiconductors, as one sees in nanogenerators and the nanopiezotronics.

Calculations based on the Lippman[13] theory have been carried out for bent piezoelectric nanowires, with an analytical solution for the electric potential derived. The Lippman theory can be used to describe bent piezoelectric nanowires when the donor concentration is extremely low, so that the conductivity can be neglected. However, the as-grown ZnO nanowires are typically n-type due to unavoidable point defects.[14−20] For semiconductor materials with a significant amount of free electrons, the Lippman theory cannot be directly applied, because the free charge carriers are able to distribute all over the material. The statistics of electrons/holes must be considered besides the phenomenological thermodynamics. The main objective of this paper is to present a macroscopic-statistical model of piezoelectricity in a laterally bent semiconductive nanowire by considering its moderate conductivity in a normal doping range. To be specific, we will calculate the electric potential when the thermodynamic equilibrium among free charge carriers is achieved. For applications that directly utilize the piezoelectric potential as the driving force to produce electric power,[7] such as the piezoelectric nanogenerators, the results could provide a more realistic picture for their operation mechanism. For piezotronics[21] devices which use the piezoelectric potential to modulate the charge transport properties,[10] the results will be a good starting point to study the quasi-static charge transport process. Although the calculations in this

* Corresponding author, zhong.wang@mse.gatech.edu.

10.1021/nl803547f CCC: $40.75
Published on Web 02/03/2009

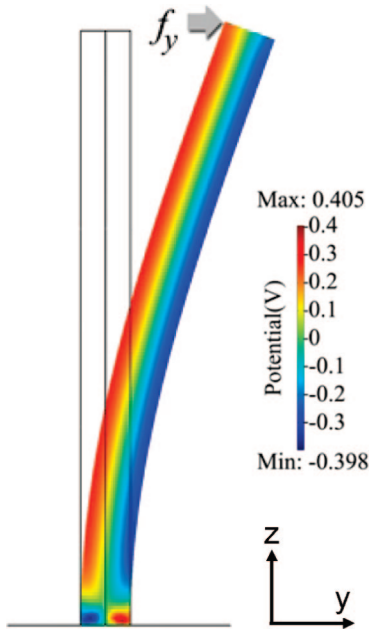

Figure 1. Piezoelectric potential distribution across the center of a ZnO nanowire that is assumed to be an insulator. The coordinate system used for the calculation is also defined. The wire is approximated as a cylinder, with radius a and length l. The nanowire is well-affixed on the substrate. The external force f_y is exerted at the top, while the boundary traction due to f_y is supposed to be uniform across the top surface. The red side is the positive side, and the blue side is the negative side. The bottom reverse region is also plotted.

paper are conducted exclusively for n-type ZnO nanowires, the methodology is directly applicable to any devices with a similar design, as long as the building material is piezoelectric and semiconductive.

Theoretical Frame. We assume that a ZnO nanowire is epitaxially grown along the c axis on a single crystal substrate, as shown in the schematic of Figure 1. The color plot of electric potential in Figure 1 is based on a previous calculation using the Lippman theory,[4] where the red side is positive and the blue side is negative.[22] The wire is laterally bent by a force f_y exerted at the top. Previous results indicated that, for a ZnO NW with zero free charge carrier density, the tensile surface would show a positive piezoelectric potential and the compressive side would show a negative potential. (In this context, by "piezoelectric potential" we mean that the potential is created by the polarizations of anions and cations in the NW; these charges cannot freely move as long as the strain is preserved.) In this paper, we will consider the finite concentration of donors and free charge carriers in ZnO.

In order to focus on the core physics by preventing the digression to the less relevant problems about the interface heterojunctions, we assume that the substrate is also made of ZnO. Such a situation occurs for the ZnO nanowires grown on GaN substrates via the VLS method,[23] because a thin ZnO film or ZnO walls usually form beneath the nanowires. Our task is to calculate the piezoelectric potential when thermodynamic equilibrium is achieved in the laterally bent nanowires.

It is well-known that when free electrons/holes are present in a piezoelectric material, the carriers will redistribute due to the electric field established by the polarization. One famous application of such a redistribution effect is in the GaN/AlGaN HEMTs, where electrons are accumulated at the heterojunction to create a two-Dimensional Electron Gas (2DEG).[11] For piezoelectric nanowire applications,[7,8] the mechanical behavior is more complicated, but the physical pictures are essentially the same. Instead of using a fully coupled constitutive equation,[13] we only write the mechanical equilibrium and the direct piezoelectric effect:

$$\begin{cases} \sigma_p = c_{pq}\varepsilon_q \\ D_i = e_{iq}\varepsilon_q + \kappa_{ik}E_k \end{cases} \tag{1}$$

where σ is the stress tensor, ε is the strain, $\vec{E}$ is the electric field, and $\vec{D}$ is the electric displacement. κ_{ik} is the dielectric constant, e_{iq} is the piezoelectric constant, and c_{pq} is the mechanical stiffness tensor. The Voigt−Nye notation[24] is used. Substituting the second equation into Gauss's law, we get the equation for the electric field

$$\nabla \cdot \vec{D} = \frac{\partial}{\partial x_i}(e_{iq}\varepsilon_q + \kappa_{ik}E_k) = \rho_e^{(b)} = ep - en + eN_D^+ - eN_A^- \tag{2}$$

where p is the hole concentration in the valance band, n is the electron concentration in the conduction band, N_D^+ is the ionized donor concentration, and N_A^- is the ionized acceptor concentration. Because the as-grown ZnO NWs are usually n-typed, we adopt $p = N_A^- = 0$. By introducing

$$\vec{D}^R = e_{kq}\varepsilon_q \hat{i}_k \tag{3.1}$$

as the polarization due to piezoelectricity and

$$\rho^R = -\nabla \cdot \vec{D}^R \tag{3.2}$$

as the corresponding piezoelectric charge, eq 2 can be rewritten for the electric potential φ

$$\kappa_{ik}\frac{\partial^2}{\partial x_i \partial x_k}\varphi = -(\rho^R - en + eN_D^+) \tag{4}$$

The surface charge due to piezoelectricity is calculated by $\Sigma^R = -\vec{n}\cdot\Delta\vec{D}^R$, where $\Delta\vec{D}^R$ is the change of $\vec{D}^R$ astride the material surface and $\vec{n}$ is the normal to the surface. For simplicity, we have ignored the surface charges introduced by polar surfaces of ZnO.

The redistribution of electrons under thermodynamic equilibrium is given by the Fermi−Dirac statistics

$$n = N_c F_{1/2}\left(-\frac{E_c(\vec{x}) - E_F}{kT}\right) \tag{5.1}$$

$$N_c = 2\left(\frac{2\pi m_e kT}{h^2}\right)^{3/2} \tag{5.2}$$

where the conduction band edge $E_c(\vec{x})$ is a function of space coordinates. N_c, the effective state density of conduction band, is determined by the effective mass of conduction band electrons m_e and the temperature T. Due to the large strain, the deformation potential might be important. To be specific, the band edge shift ΔE_c is the sum of the electrostatic energy part and the deformation potential part

$$E_c - E_{c_0} = \Delta E_c = -e\varphi + \Delta E_c^{\text{deform}} = -e\varphi + a_c \frac{\Delta V}{V} \quad (6)$$

where E_{c_0} is the conduction band edge of a free-standing un-deformed semiconductor material; $\Delta E_c^{\text{deform}} = a_c \Delta V/V$ is the band edge shift due to the deformation potential,[25] which is proportional to the relative volume change $\Delta V/V$, and a_c is the deformation potential constant. Finally, the activation process of the donors is given by

$$N_D^+ = N_D \frac{1}{1 + 2\exp\left(\frac{E_F - E_D}{kT}\right)} \quad (7)$$

where $E_D(\vec{x}) = E_C(\vec{x}) - \Delta E_D$ is the position-dependent donor energy level. The constant ΔE_D is the activation energy of the donors. N_D is the concentration of the donors.

With eqs 4−7, the piezoelectric potential in a bent ZnO nanowire with moderate charger carrier density can be calculated. It should be pointed out that eqs 4−7 are valid only when the system dimension is not too small. For small systems, strong confinement requires quantum mechanical considerations due to discrete bound states. Such an elaboration in theory is necessary for 2DEG in GaN/AlGaN HEMTs, in which the quantum effect is important.[11] In the following section we will conduct the calculation for nanowires with diameter ~50 nm or larger, where nonquantum mechanical calculation is still acceptable. Such a size range is typical in experiments.[7]

The Fermi level E_F is flat all over the bent semiconductor nanowire when thermodynamic equilibrium is assumed. Because the nanowires are assumed to be grown on a substrate whose dimension is much larger than the nanowires, the substrate can be taken as a vast reservoir that pins the Fermi level. In this paper we assume that the substrate is made of the same material as the nanowire itself. For nanowires making direct heterogeneous junctions with the substrate, depletion regions or charge-accumulation regions may form at the bottom junctions, which will not be elaborated in this paper.

When negligible donor concentration is assumed, the electric field in a bent piezoelectric nanowire has been solved analytically,[4] with the piezoelectric potential shown to be independent of the coordinate z in a cylindrical coordinate system. Due to the Saint-Venant principle approximation, the analytical solution[4] is valid only for places that are not too close to the root of the wire. At the root, finite element analysis (FEA) showed the existence of a potential reversed region if no donor concentration is considered (as seen in the bottom part in Figure 1).[4] It can be proved that the piezoelectric charge ρ^R at the bottom region forms an electric dipole, whose potential decays as fast as $1/r^2$ (see Appendix). Therefore it is legitimate to ignore the bottom reverse regions when calculating the electric potential in the nanowire under zero donor concentration assumption.[4] However, when electrons in conduction band come into the play, the piezoelectric polarization charges might be screened by the free charge carriers. Owing to the screening effect, the potential due to the bottom region might decay as slow as $1/r$. Therefore one needs to model both NW and the substrate. Nevertheless, the main purpose of this paper is to investigate the piezoelectric behavior inside the nanowire itself. Instead of elaborating into the details of the bottom reversed potential region, we model the bottom region mainly to avoid missing its contribution to the potential in the nanowire. A more detailed investigation about the bottom reverse region is suggested for future research.

Numerical Results and Discussion. We use the finite element method (FEM) to solve the nonlinear partial differential equation posed by eqs 4−7. Symmetry is used so we only need to solve for the half-space of $x > 0$. Solution in the other half of space can be immediately derived by using the mirror symmetry of the $x = 0$ plane. In order to help the convergence, we first linearize eq 5.1 and eq 7 by introducing an extreme case of ultrahigh temperature T_{high}. For the convenience of calculations as presented in eq 5.1 and eq 7, we define the following variables

$$\eta = -\frac{E_c(\vec{x}) - E_F}{kT}$$

and

$$\eta_D = \frac{E_F - E_D}{kT} = \eta + \frac{\Delta E_D}{kT} \quad (8)$$

When $T = T_{\text{high}}$ is large, η and η_D are no longer position-dependent; the problem is thus linearlized for easy solution. As a convergence tool, T_{high} by itself is not required to have realistic physical meaning. Nevertheless, the solutions under high temperature $T = T_{\text{high}}$ do evince some meaningful insight in physics. In fact, $\eta \approx \eta_D \approx \ln(N_D/N_C)$ when $T = T_{\text{high}}$; therefore $N_D^+ = n$ and equ 4 would give an unscreened solution as though there were neither donors nor free charge carriers in ZnO. As the system "cools down" from T_{high} to the realistic temperature, the equations become more and more nonlinear. The value of η dictates how degenerate the system is, with $\eta > -3$ being regarded as the highly degenerate case. As we will see later in the results, the problem will involve some degree of degeneracy even when the donor concentration is relatively low. This is analogous to the 2DEG regions in GaN/AlGaN HEMTs,[11] where electrons accumulate even when the local doping level is small.

Despite more than a decade of investigations, the nature of the unintentionally introduced donors in ZnO crystal has been controversial.[15−20,26] Various mechanisms have been proposed, and reports about multiple shallow donor levels can be found in the literature with reported donor activation energies ranging from 30 to 60 meV.[15,18,27] Instead of complicating the theory with multiple donor levels, we only consider one single donor level with $\Delta E_D = 35$ meV.[18] It should be pointed out that the methodology and qualitative conclusions in this paper do not rely on the exact number of shallow donor levels and/or their activation energies. We also neglect the deep donor levels or surface states which may exist in ZnO nanowire[28,29] to keep focusing on the central physics. Later we will see that the band edge shift is generally less than 0.5 eV except for a small region in the negative side of the bottom reverse region. The activation energy for the deep donor levels is reported to be much larger than 0.5 eV in the scale of kT.[29] Therefore the neglect of deep donors should not result in a significant error.

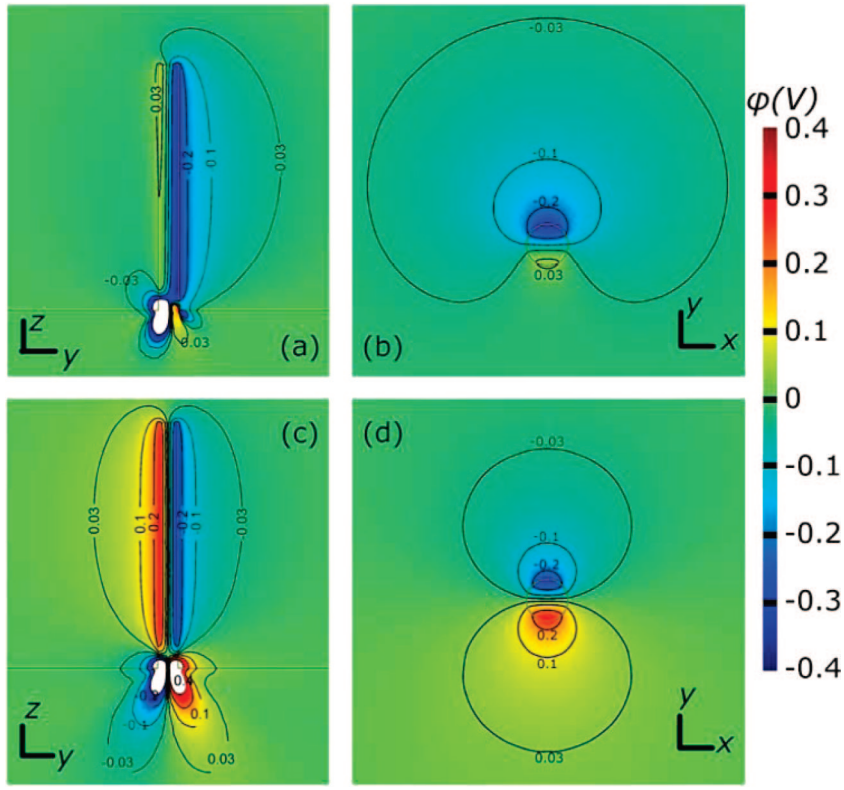

Figure 2. Plot of calculated piezoelectric potential φ for $N_D = 1 \times 10^{17}$ cm^{-3}. For easy plot, the bending shape of the nanowire is not presented. Besides the color plot, equipotential contours for $\varphi = -0.4, -0.2, -0.1, -0.03, 0.03, 0.1, 0.2$, and 0.4 V are also superimposed. The dimension of the nanowire is $a = 25$ nm and $l = 600$ nm and the external force is $f_y = 80$ nN. (a) Plot of φ for $T = 300$ K at a cross section of $x = 0$. The blank region at the bottom is the region where $\varphi < -0.4$ V. The detail in this region is oversaturated for display purposes to optimize the color scale in order to show φ in the nanowire. In this paper, we mainly focus on the behavior in the nanowire and will leave the details about the bottom reverse region for future research. (b) Cross section plot of the electric potential for $T = 300$ K at the height $z = 400$ nm. Here only half of the space $x > 0$ is calculated using the mirror symmetry of $x = 0$ plane. The plot in the $x < 0$ region is derived by a simple reflection of the solution in the $x > 0$ region. (c and d) Calculation for an extremely high temperature case of $T = T_{high} = 300000$ K in reference to the result received from nanowires without doping. Again the extreme peaks are oversaturated. (c) The cross section $x = 0$. (d) The cross section plot of the electric potential at height $z = 400$ nm.

In contrast to the lack of a universally accepted activation energy and model for the donors, the ZnO band gap of ~3.4 eV has long been established.[30] Our model does not involve the data on band gap except the fact that the wide band gap is larger than the possible band shift $\Delta E_c = -e\varphi + \Delta E_c^{deform}$. Therefore, the Fermi level is always far away from the valence band and we do not need to consider holes or acceptors.[31]

The material constants for ZnO used in the calculations are as follows: Young's modulus $E = 129.0$ GPa and Poisson ratio $\nu = 0.349$;[2] relative dielectric constants $\kappa_\perp^r = 7.77$, $\kappa_\parallel^r = 8.91$,[2] and the piezoelectric constants $e_{31} = -0.51 C/m^2$, $e_{33} = 1.22 C/m^2$, $e_{15} = -0.45 C/m^2$.[2] Effective mass is $m^* = 0.28 m_0$,[32] and deformation potential constant is $a_c = -6.05$ eV.[25] The change of effective mass due to strain is not considered. The nanowire is geometrically approximated as a cylinder, with radius $a = 25$ nm, and length $l = 600$ nm. The external force is $\vec{f} = f_y \vec{e}_y$, $f_y = 80$ nN, uniformly applied at the top surface of the nanowire in a direction $\vec{e}_y$ perpendicular to the nanowire axis. The geometry and the external force are adopted as typical estimated numbers in an atomic force microscopy (AFM) based piezoelectric potential detection experiment.[7] Since the donor concentration N_D varies according to the growth conditions with a typical concentration around 10^{17} cm^{-3},[15,18] our calculations are made for typical values around $N_D = 1 \times 10^{17}$ cm^{-3}.

Figure 2a shows the equal-potential lines for $N_D = 1 \times 10^{17}$ cm^{-3} and $T = 300$ K on the cross section plane $x = 0$, which is right through the axis of the nanowire. Figure 2b gives the equal-potential lines on a cross section perpendicular to the nanowire axis and at a height of $z = 400$ nm. The electrostatic calculation is done under a small strain assumption, in which the difference between the Lagrangian reference frame and Eulerian reference frames is neglected. For comparison purposes, the results received under the unrealistic temperature of $T = T_{high} = 300000$ K is also plotted in panels c and d of Figure 2, which correspond to the situation when ZnO were an insulator without any free charge carriers. The result for $T = T_{high}$ is exactly the same as that given by the analytical solution in ref 4.

The electric potential maximum in the positive side of the nanowire is significantly reduced from ~0.3 V in Figure 2d, which corresponds to an insulator case, to less than 0.05 V in Figure 2b, which considers the moderate doping in ZnO. On the other hand, the potential in the compressed side (negative potential side) is very well preserved. This is consistent with the experimental observation that only negative pulses are observed in an AFM-based nanogenerator

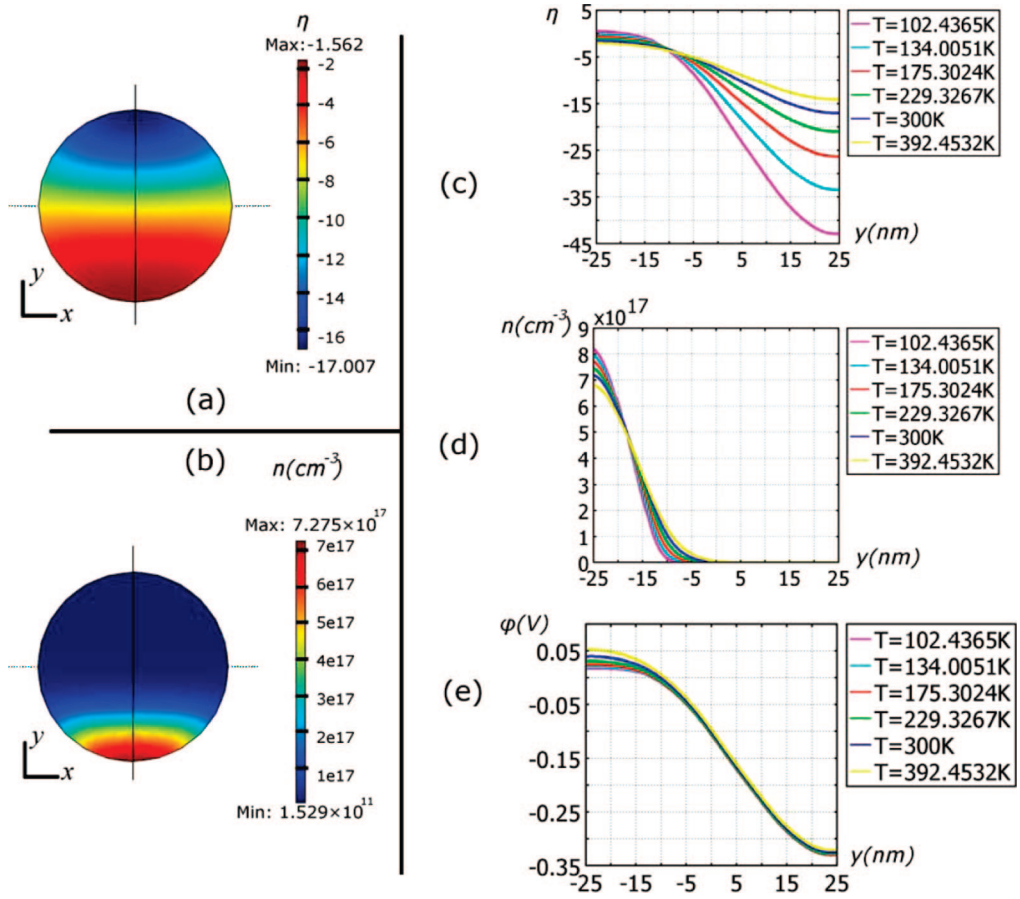

Figure 3. (a and b) Cross section color plot of parameters η (a) and local electron density n (b) for $N_D = 1 \times 10^{17}$ cm^{-3} and $T = 300$ K at the height $z = 400$ nm. Here only half of the space $x > 0$ is calculated using the mirror symmetry of $x = 0$ plane. The plot in the $x < 0$ region is derived by a simple reflection of the solution in the $x > 0$ region. (c−e) Line plot of η, n, and φ under different temperatures along the diameter in (a) and (b). The horizontal axis is the y-coordinate.

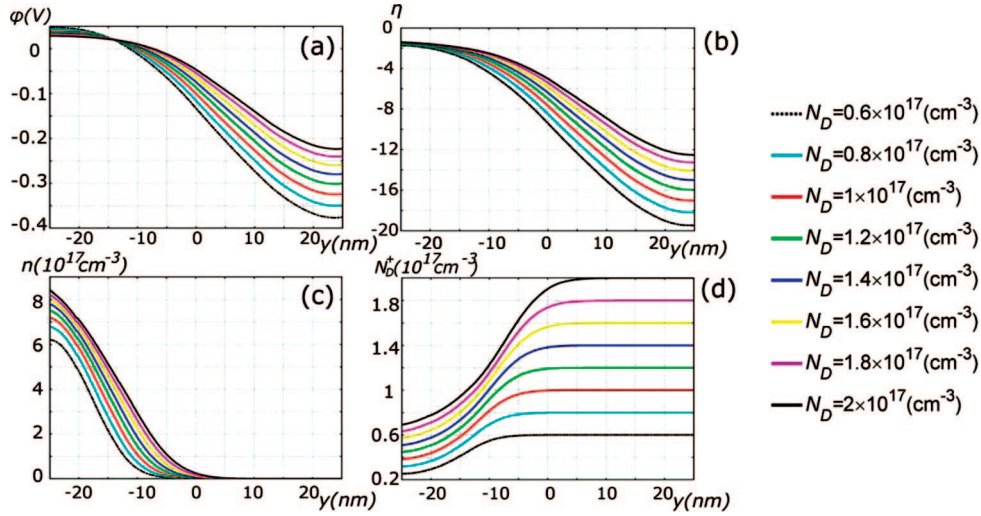

Figure 4. (a) Piezoelectric potential φ, (b) parameter η, (c) free electron concentration n, and (d) activated donor center concentration N_D^+ for different donor concentrations 0.6×10^{17} cm^{-3} $\leq N_D \leq 2.0 \times 10^{17}$ cm^{-3}. The dimension of the nanowire is $a = 25$ nm, $l = 600$ nm and the external force is f_y=80 nN. $T = 300$ K. The line plot is along the diameter in Figure 2b and Figure 3a.

experiment using n-type ZnO nanowires.[7] It is also consistent with the observation that the output negative potential peak appears only when the AFM tip touches the compressed side of the nanowire. The decrease of positive potential in this model is due to the in-flow of electrons from the substrate where free charges are abundant. When positive polarization charges $\rho^R > 0$ try to create a positive local potential $\varphi > 0$, it would result in a downward bending of the local conduction band. When η gets close to or even bigger than zero, a large amount of free electrons would be injected from the substrate reservoir into the nanowire to screen the positive potential.

In the negative potential side (compressed side of the nanowire), however, free charge carriers are depleted due to a large negative value of η, leaving only $\rho^R + eN_D^+$ as the net charge in eq 4. Let us use the analytical equation derived in ref 4 to evaluate the concentration of ionic polarization charge. Substituting $a = 25$ nm, $l = 600$ nm, and $f_y = 80$ nN into

$$\rho^R = \frac{f_y}{I_{xx}E}[2(1+\nu)e_{15} + 2\nu e_{31} - e_{33}]y$$

where $I_{xx} = (\pi/4)a^4$,[4] one gets the typical piezoelectric polarization charge density $\rho_R{}^{y=a}/e \sim -8.8 \times 10^{17}$ cm^{-3} near the wire surface $y = a$, where e is the charge of a single electron. When $N_D = 1 \times 10^{17}$ cm^{-3}, ρ_R cannot be totally screened in the negative side even if all of the electrons are depleted because N_D is much smaller than $\rho_R{}^{y=a}/e$. For a nanowire with a very high donor concentration $N_D > 10^{18}$ cm^{-3}, total neutralization with $\varphi \approx 0$ could occur everywhere. Namely, a NW with a high concentration of free charge carriers is expected to exhibit a very small piezoelectric potential. This result agrees to the experimental measurement of a nanogenerator under the illumination of UV light.[5] In reality, the doping level in as-grown unintentionally doped ZnO nanowires is much smaller than 10^{18} cm^{-3}.

The band edge shift ΔE_c comprises of two parts: electric potential part and the deformation potential part. The Saint−Venant solution for stress in the nanowire is $\sigma_{zz} = -(f_y/I_{xx})y(l - z)$, $\sigma_{xx} = \sigma_{yy} = 0$,[4] therefore

$$|\Delta E_c^{\text{deform}}| = a_c|\Delta V/V| = a_c|Tr(\varepsilon)|$$
$$= a_c\left|\frac{1-2\nu}{E}Tr(\sigma)\right| = \left|-a_c\frac{1-2\nu}{E}\frac{f_y}{I_{xx}}y(l-z)\right| <$$
$$a_c\frac{1-2\nu}{E}\frac{f_y}{I_{xx}}\cdot a\cdot l = 55 \text{ meV}$$

As a posterior observation, this value is much smaller than the negative side value of $|e\varphi|$; therefore the deformation potential could have been neglected before the calculation if the potential magnitude in the negative side is the main concern. It also indicates that the negative potential observed in experiments[7] should not be due to the deformation potential band-structure shift but mainly due to piezoelectric effect.

Degeneracy is significant in the screened positive side as seen in the η plot in Figure 3a. The degeneracy in the charge accumulation region is due to the piezoelectric effect but not due to large donor concentration or low temperature. Before deformation, $\eta = \eta_0 = -3.77$ for $N_D = 1 \times 10^{17}$ cm^{-3} at $T = 300$ K; this is below the degeneracy criterion. In order to investigate how temperature affects the free charge carrier distribution and the final electric potential, we plotted n, η, and φ for different temperatures (Figure 3, curves c−e). The variance of n, η, and φ is small for temperatures in a range of 100 K $< T <$ 400 K. The free carrier concentration is $n \sim 10^{15}$ cm^{-3} in the depletion region and $n \sim \rho_R/e + N_D \sim 10^{18}$ cm^{-3} in the charge accumulation region as seen in Figure 3b. The boundary between the charge accumulation region and the depletion region is quite sharp. We notice that the width of the charge accumulation region is much smaller than the wire diameter a, which implies strong confinement of the conduction band electrons. This strong confinement might result in stronger quantum effect than that seen in the NW's undeformed state.

In order to investigate how the variance of N_D affects the piezoelectric potential, we plot the (a) electric potential φ, (b) parameter η, (c) free electron concentration n, and (d) activated donor center concentration N_D^+ for different donor concentrations 0.6×10^{17} cm^{-3} $< N_D <$ 2.0×10^{17} cm^{-3} under $T = 300$ K in Figure 4. It is seen that the electric potential φ is rather insensitive to the donor concentration in this regime. However, it is expected that φ will be completely neutralized when $N_D > 10^{18}$ cm^{-3}, as we have already discussed. In the $y < 0$ region (stretched side of the nanowire), degeneracy is always significant due to large η value (Figure 4b). Therefore, electrons will be accumulated in the $y < 0$ side as seen in Figure 4c and depleted in the compressed side of the nanowire ($y > 0$). On the other hand, the donor centers are not well activated in the $y < 0$ side as seen in Figure 4d, which makes the local electric charge density $\rho^R - en + eN_D^+$ in the $y < 0$ side even smaller.

Summary. In summary, the behavior of free charge carriers in a bent piezoelectric ZnO nanowire is investigated under a thermodynamic equilibrium condition. By assuming a flat Fermi level and a homojunction between the ZnO nanowire and the substrate, we arrived at a conclusion that, for a doping level of $N_D = 1 \times 10^{17}$ cm^{-3}, the compressed side of the nanowire preserves the negative piezoelectric potential, while the stretched side with positive potential is partially screened by free electrons. Charge carriers are accumulated at the stretched side of the ZnO nanowire, and the compressive side is largely depleted. Degeneracy in the positive side of the nanowire is significant, but the temperature dependence of the potential profile is weak in the temperature range of 100 K $< T <$ 400 K. Our results support the mechanism proposed and demonstrated experimentally for piezoelectric nanogenerators[7] and nanopiezotronics.[7,21]

Acknowledgment. Research supported by DARPA (Army/AMCOM/REDSTONE AR, W31P4Q-08-1-0009).

Appendix. Analytical Consideration of the Reversed Electrostatic Potential at the Bottom of the Nanowire. To prove the existence of the bottom reverse region and calculate the amount of charge therein, let us investigate the piezoelectric polarization charge ρ^R, which is defined by eq 3. By doing this we will be able to calculate the total amount of piezoelectric charge if zero donor concentration is assumed. We suppose that the deformation is not too large; therefore the detailed difference between the Lagrangian and Eulerian coordinate systems can be neglected when we investigate the electrostatics as seen in Figure 5. To be specific, we will consider the problem in a material coordinate system (x,y,z). For simplicity, we consider a case that has no doping, i.e., zero conductivity. It is easy to see that the piezoelectric polarization charge ρ^R should be antisymmetric with respect to y

$$\rho^R(x,-y,z) = -\rho^R(x,y,z) \tag{9}$$

Consider a domain V_L (dotted part in Figure 5), whose boundary ∂V_L consists of four parts: neutral plane $y = 0$, substrate surface $z = 0$, nanowire surface, and an imaginal quad-spherical surface $\Sigma_{R_0} = \{(x,y,z)|x^2 + y^2 + z^2 = R_0^2, y \le 0, z \le 0\}$ deep in the substrate with radius $R_0 \gg l$. Consider $Q_{T,\text{Left}}$, which is defined as the total charge inside V_L and on ∂V_L

$$Q_{T,\text{Left}} = \iiint_{V_L \cup \partial V_L} \rho^R \mathrm{d}V = -\iiint_{\substack{x^2+y^2 \le R_0^2 \\ y \le 0}} \nabla \cdot \vec{D}^R \mathrm{d}V = -\iint_{\Sigma_{R_0}} \vec{D}^R \cdot \mathrm{d}\vec{S} - \iint_{\Sigma_y} \vec{D}^R \cdot \mathrm{d}\vec{S} \tag{10}$$

where Σ_y is the $y = 0$ part of ∂V_L. The last step in eq 10 is based on the fact that $\vec{D}^R = 0$ outside the ZnO material and a simple application of the divergence theorem.

Let us first consider the Σ_y part in eq 10. By eq 3.1 and eq 1

$$\vec{D}^R \cdot \mathrm{d}\vec{S} = \vec{D}^R \cdot \hat{e}_y \, \mathrm{d}A = D_y^R \, \mathrm{d}A = e_{15}\gamma_{yz} \, \mathrm{d}A = \frac{2(1+\nu)}{E} e_{15}\sigma_{yz} \, \mathrm{d}A$$

Therefore

$$\iint_{\Sigma_y} \vec{D}^R \cdot \mathrm{d}\vec{S} = \frac{2(1+\nu)}{E} e_{15} \iint_{\Sigma_y} \sigma_{yz} \mathrm{d}A = \frac{2(1+\nu)}{E} e_{15} \left(\iint_{\Sigma_y} \mathrm{d}\vec{S} \cdot \bar{\bar{\sigma}} \right) \cdot \hat{e}_z \tag{11}$$

where $\bar{\bar{\sigma}} = \sigma_{ij}\hat{e}_i \otimes \hat{e}_j$ is the stress tensor without using the Voigt−Nye convention. On the other hand, since the only external force is $f_y\vec{e}_y$ on the top surface, the mechanical equilibrium condition requires

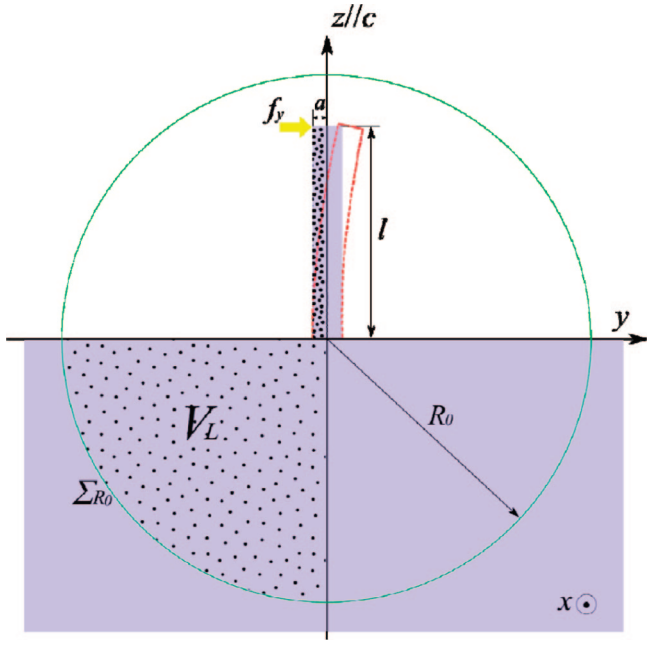

Figure 5. The figure used to calculate the charge in the bottom reverse region. The total charge in domain V_L is proved to be zero.

$$\left[\iint_{\Sigma_y} \mathrm{d}\vec{S} \cdot \bar{\bar{\sigma}} + \iint_{\Sigma_{R_0}} \mathrm{d}\vec{S} \cdot \bar{\bar{\sigma}} \right] \cdot \hat{e}_z = 0 \tag{12}$$

Therefore

$$-\iint_{\Sigma_y} \vec{D}^R \cdot \mathrm{d}\vec{S} = \frac{2(1+\nu)}{E} e_{15} \left(\iint_{\Sigma_{R_0}} \mathrm{d}\vec{S} \cdot \bar{\bar{\sigma}} \right) \cdot \hat{e}_z \tag{13}$$

Now consider the far region $r \sim R_0$ in a spherical coordinate(r,θ,ϕ). The mechanical behavior in the substrate is a Boussinesq−Cerruti problem which involves a concentrated load.[33] The asymptotic behavior of σ_{ij} can be expressed as $\sigma_{ij} = (f_y)/(r^2)\psi_{ij}^{\sigma}(\theta,\phi)$, where $\psi_{ij}^{\sigma}(\theta,\phi)$ is the dimensionless angular dependence. The leading term is r^{-2} when there is a net force f_y component in the concentrated load. The contribution due to a pure torque decays faster as r^{-3} thus can be neglected. With the unit normal vector $\hat{n} = n_i\hat{e}_i$ on Σ_{R_0},

$$\begin{aligned}
-\iint_{\Sigma_y} \vec{D}^R \cdot \mathrm{d}\vec{S} &= \frac{2(1+\nu)}{E} e_{15} \left(\iint_{\Sigma_{R_0}} \mathrm{d}\vec{S} \cdot \bar{\bar{\sigma}} \right) \cdot \hat{e}_z \\
&= \frac{2(1+\nu)}{E} e_{15} \iint_{\Sigma_{R_0}} \sigma_{i3} n_i \, \mathrm{d}A \\
&= \frac{2(1+\nu)}{E} e_{15} \int_{\pi/2}^{\pi} \mathrm{d}\theta \int_{\pi}^{2\pi} \mathrm{d}\phi R_0^2 \sin\theta \left[\sin\theta \cos\phi \frac{f_y}{R_0^2} \psi_{13}^{\sigma}(\theta,\phi) + \right. \\
&\left. \sin\theta \sin\phi \frac{f_y}{R_0^2} \psi_{23}^{\sigma}(\theta,\phi) + \cos\theta \frac{f_y}{R_0^2} \psi_{33}^{\sigma}(\theta,\phi) \right] \\
&= \frac{2(1+\nu)}{E} e_{15} f_y c_{\text{angular}}
\end{aligned} \tag{14}$$

where the dimensionless constant

$$c_{\text{angular}} = \int_{\pi/2}^{\pi} \mathrm{d}\theta \int_{\pi}^{2\pi} \mathrm{d}\phi [\sin^2\theta \cos\phi \psi_{13}^{\sigma}(\theta,\phi) + \sin^2\theta \sin\phi \psi_{23}^{\sigma}(\theta,\phi) + \sin\theta \cos\theta \psi_{33}^{\sigma}(\theta,\phi)]$$

does not dependent on the values of a,l, or f_y. It should be noted that with the Boussinesq−Cerruti theory, c_{angular} can be calculated. However, in this paper we do not elaborate on the exact value of c_{angular} but only use the simple fact that c_{angular} is independent of the wire shape and the magnitude of the external force. We also note that c_{angular} should not be much bigger than 1.

On the other hand, it has been proved that, in the nanowire, the piezoelectric polarization charge is,[4]

$$\rho^R = \frac{f_y}{I_{xx}E}[2(1+\nu)e_{15} + 2\nu e_{31} - e_{33}]y \tag{15}$$

where $I_{xx} = \int_{\text{CrossSection}} x^2 \, \mathrm{d}A = (\pi/4)a^4$. This solution is valid for places not too close to the substrate, where by "not too close" it means $z \gg a$. The surface charge density $\Sigma^R = -\vec{n}\cdot\Delta\vec{D}^R$ due to piezoelectric polarization on the wire surface has been proved to be 0.[4]

Integrating eq 15 gives the total charge in the $y < 0$ part of the nanowire

$$Q_{\text{wire,Left}} = -\frac{8}{3\pi} \frac{2(1+\nu)e_{15} + 2\nu e_{31} - e_{33}}{E} \frac{l}{a} f_y \tag{16}$$

While c_{angular} is a constant independent of a, l, or f_y, the nanowire has a large aspect ratio $l/a \gg 1$. Therefore, by comparing eq 14 and eq 16

$$\left|-\int\int_{\Sigma_y} \vec{D}^R \cdot d\vec{S}\right| \ll |Q_{\text{wire,Left}}|$$

A similar conclusion can be drawn for the first term in equation (10) by similar analysis, namely,

$$\left|-\int\int_{\Sigma_{R_0}} \vec{D}^R \cdot d\vec{S}\right| \ll |Q_{\text{wire,Left}}|$$

Therefore, there must be a bottom reverse region with a negative (e_{33} is positive while e_{31} and e_{15} are negative) piezoelectric polarization charge $Q_{\text{BRG,Left}}$

$$\begin{aligned} Q_{\text{BRG,Left}} &= Q_{\text{T,Left}} - Q_{\text{wire,Left}} \\ &= -\int\int_{\Sigma_{R_0}} \vec{D}^R \cdot d\vec{S} - \int\int_{\Sigma_y} \vec{D}^R \cdot d\vec{S} - Q_{\text{wire,Left}} \\ &= \frac{8}{3\pi} \frac{2(1+\nu)e_{15} + 2\nu e_{31} - e_{33}}{E} \frac{l}{a} f_y \cdot \left[1 + O\left(\frac{a}{l}\right)\right] \\ &\approx -Q_{\text{wire,Left}} \end{aligned} \tag{17.1}$$

Due to the antisymmetry in eq (9), there is another bottom reverse region on the $y > 0$ side with a positive piezoelectric polarization charge,

$$\begin{aligned} Q_{\text{BRG,Right}} &= -\frac{8}{3\pi} \frac{2(1+\nu)e_{15} + 2\nu e_{31} - e_{33}}{E} \frac{l}{a} f_y \cdot \left[1 + O\left(\frac{a}{l}\right)\right] \\ &\approx -Q_{\text{wire,Right}} \end{aligned} \tag{17.2}$$

By deriving eqs 17.1 and 17.2 we also confirmed the existence of the bottom reverse region. When the donor concentration is zero, the bottom reverse region makes an electric dipole. When free charge carriers are available, a net charge might accumulate in the bottom reverse region.

References

(1) Lieber, C. M.; Wang, Z. L. *MRS Bull.* **2007**, *32* (2), 99–108.
(2) Lu, W.; Lieber, C. M. *J. Phys. D: Appl. Phys.* **2006**, *39* (21), R387−R406.
(3) Gao, P. X.; Song, J. H.; Liu, J.; Wang, Z. L. *Adv. Mater.* **2007**, *19* (1), 67–72.
(4) Gao, Y.; Wang, Z. L. *Nano Lett.* **2007**, *7* (8), 2499–2505.
(5) Liu, J.; Peng, F.; Song, J. H.; Wang, X. D.; Lao, C. S.; Tummala, R.; Wang, Z. L. *Nano Lett.* **2007**, *8* (1), 328–332.
(6) Wang, X. D.; Song, J. H.; Jiu, J.; Wang, Z. L. *Science* **2007**, *316*, 102–105.
(7) Wang, Z. L.; Song, J. H. *Science* **2006**, *312* (5771), 242–246.
(8) Wang, X. D.; Zhou, J.; Song, J. H.; Liu, J.; Xu, N. S.; Wang, Z. L. *Nano Lett.* **2006**, *6* (12), 2768–2772.
(9) He, H.; Hsin, C. L.; Liu, J.; Chen, L. J.; Wang, Z. L. *Adv. Mater.* **2007**, *19* (6), 781.
(10) Zhou, J.; Gu, Y. D.; Fei, P.; Mai, W. J.; Gao, Y. F.; Yang, R. S.; Bao, G.; Wang, Z. L. *Nano Lett.* **2008**, *8* (9), 3035–3040.
(11) Sacconi, F.; Di Carlo, A.; Lugli, P.; Morkoc, H. *IEEE Trans. Electron Devices* **2001**, *48* (3), 450–457.
(12) Lu, J. G.; Ye, Z. Z.; Zhang, Y. Z.; Liang, Q. L.; Fujita, S.; Wang, Z. L. *Appl. Phys. Lett.* **2006**, *89* (2), 023122.
(13) Landau, L. D.; Lifshitz, E. M.; Pitaevskii, L. P., *Electrodynamics of continuous media*, 2nd ed.; Pergamon: New York, 1984.
(14) Gorelkinskii, Y. V.; Watkins, G. D. *Phys. Rev. B* **2004**, *69* (11), 115212.
(15) Look, D. C.; Farlow, G. C.; Reunchan, P.; Limpijumnong, S.; Zhang, S. B.; Nordlund, K. *Phys. Rev. Lett.* **2005**, *95* (22), 225502.
(16) Van de Walle, C. G. *Phys. Rev. Lett.* **2000**, *85* (5), 1012–1015.
(17) Cox, S. F. J.; Davis, E. A.; Cottrell, S. P.; King, P. J. C.; Lord, J. S.; Gil, J. M.; Alberto, H. V.; Vilao, R. C.; Duarte, J. P.; de Campos, N. A.; Weidinger, A.; Lichti, R. L.; Irvine, S. J. C. *Phys. Rev. Lett.* **2001**, *86* (12), 2601–2604.
(18) Hofmann, D. M.; Hofstaetter, A.; Leiter, F.; Zhou, H. J.; Henecker, F.; Meyer, B. K.; Orlinskii, S. B.; Schmidt, J.; Baranov, P. G. *Phys. Rev. Lett.* **2002**, *88* (4), 045504.
(19) Shimomura, K.; Nishiyama, K.; Kadono, R. *Phys. Rev. Lett.* **2002**, *89* (25), 255505.
(20) Shi, G. A.; Stavola, M.; Pearton, S. J.; Thieme, M.; Lavrov, E. V.; Weber, J. *Phys. Rev. B* **2005**, *72* (19), 195211.
(21) Wang, Z. L. *Adv. Mater.* **2007**, *19* (6), 889–892.
(22) The color plot in Figure 1is given by the Lippman theory, where zero donor concentration is assumed and the bottom of the nanowire is assumed to be well grounded. As proved in the Appendix, the bottom reverse region does not affect the behavior in the upper part of the nanowire under a zero donor concentration assumption. In a theory about the equilibrium behavior of free charges, however, the substrate itself needs to be modeled along with the nanowire.
(23) Wang, X. D.; Song, J. H.; Liu, J.; Wang, Z. L. *Science* **2007**, *316* (5821), 102–105.
(24) Nye, J. F. *Physical Properties of Crystals*; Oxford University Press: Oxford, 1957.
(25) Shan, W.; Walukiewicz, W.; Ager, J. W.; Yu, K. M.; Zhang, Y.; Mao, S. S.; Kling, R.; Kirchner, C.; Waag, A. *Appl. Phys. Lett.* **2005**, *86* (15), 153117.
(26) Look, D. C.; Hemsky, J. W.; Sizelove, J. R. *Phys. Rev. Lett.* **1999**, *82* (12), 2552–2555.
(27) Look, D. C.; Coskun, C.; Claflin, B.; Farlow, G. C. *Physica B* **2003**, *340*, 32–38.
(28) Janotti, A.; Van de Walle, C. G. *Appl. Phys. Lett.* **2005**, *87* (12), 122102.
(29) Selim, F. A.; Weber, M. H.; Solodovnikov, D.; Lynn, K. G. *Phys. Rev. Lett.* **2007**, *99* (8), 085502.
(30) Look, D. C. *Phys. Status Solidi B* **2001**, *228* (1), 293–302.
(31) Tuomisto, F.; Ranki, V.; Saarinen, K.; Look, D. C. *Phys. Rev. Lett.* **2003**, *91* (20), 205502.
(32) Klingshirn, C. *ChemPhysChem* **2007**, *8* (6), 782–803.
(33) Soutas-Little, R. W. *Elasticity*; Dover Publications: Mineola, NY, 1999.

NL803547F